Electronic Supplementary Material (ESI) for Journal of Materials Chemistry C.

All-Acceptor Polymers with Noncovalent Interactions for Efficient Ambipolar Transistors

Zhicai Chen, [a, §] Mingguang Li, [a, §] Mengxiao Hu, [b, §] Shuang Wang, [a] Zhagen Miao, [b, c] Shen Xu, [a] Cailin Chen, [a] Huanli Dong, *[b] Wei Huang, [a] and Runfeng Chen*[a]

[a]Key Laboratory for Organic Electronics and Information Displays & Jiangsu Key Laboratory for Biosensors, Institute of Advanced Materials (IAM), Jiangsu National Synergistic Innovation Center for Advanced Materials (SICAM), Nanjing University of Posts &Telecommunications, 9 Wenyuan Road, Nanjing 210023, China

[b]Beijing National Laboratory for Molecular Sciences, Key Laboratory of Organic Solids, Institute of Chemistry, Chinese Academy of Sciences, Beijing 100190, China

[c]University of Chinese Academy of Sciences, Beijing 100049, China

Contents

1. Materials

All reagents were obtained from commercial suppliers and used as received (for example, J&K Corp. and SunaTech Inc.). Toluene and tetrahydrofuran (THF) were dried according to the standard procedures.

2. Measurements and instruments

Nuclear magnetic resonance (NMR) spectra were recorded on a Bruker Ultra Shield Plus AV400 spectrometer (^{1}H NMR 400 MHz and ^{13}C NMR 100 MHz) with $CDCl_3$ as the solvents and tetramethylsilane (TMS) as the internal standard. Matrix assisted laser desorption/ionization time-of-flight mass spectrometry (MALDI-TOF MS) measurements were carried out on a Shimadzu AXIMA-CFR mass spectrometer. Gel permeation chromatography (GPC) were carried out on Shim-pack GPC-80 X columns with THF as the eluent. Elemental analyses were performed on an Elementar Vario EL III elemental analyzer.

3. Synthetic procedure

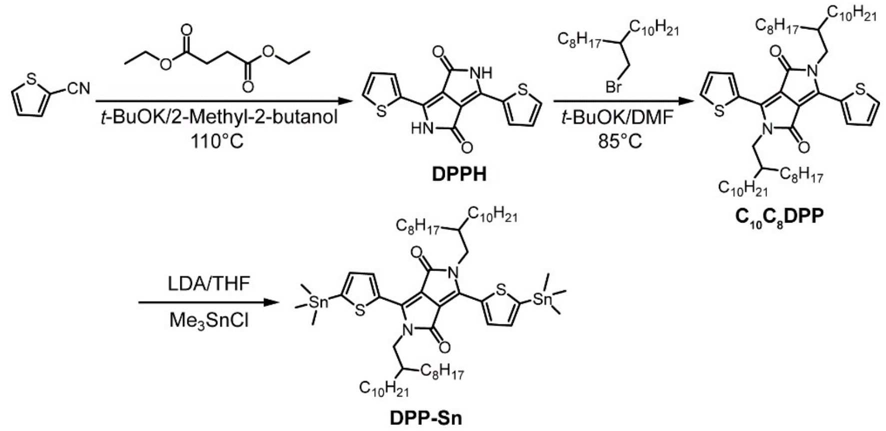

Scheme S1. The synthetic route of the monomer of **DPP-Sn**.

3,6-Di(thiophen-2-yl)-2,5-dihydropyrrolo[3,4-c]pyrrole-1,4-dione (DPPH)

Potassium *tert*-butylate (5.2 g, 46.4 mmol) was added to a round flask with argon protection. Then a solution of *t*-amyl alcohol (40 mL) and 2-thiophenecarbonitrile (5.0 g, 39 mmol) was injected by a syringe in one portion. The mixture was warmed up to 110°C, and a solution of dimethyl succinate (1.9 g, 13 mmol) in *tert*-amyl alcohol (10 mL) was dropped into slowly in 0.5 h. The reaction was kept at the same temperature for about 3 h, and then the byproduct of ethanol was distilled off and the reaction was kept for another 2 h. Then, the mixture was cooled to 65°C, diluted with 50 mL of methanol, and neutralized with acetic acid and refluxed for another 10 min. The resulting suspension was filtered, and the black filter solid was washed twice by hot methanol and water and dried in vacuum to get the coarse product, which can be used directly in next step without further purification (3.1 g, yield 79%).[1]

2,5-Bis(2-octyldodecyl)-3,6-di(thiophen-2-yl)-2,5-dihydropyrrolo[3,4-c]pyrrole-1,4-dione ($C_{10}C_8$DPP)

To a mixture of **DPPH** (1.5 g, 5 mmol), potassium *tert*-butoxide (2.3 g, 20 mmol), and dry (N, N-Dimethylformamide) DMF (40 mL) at 65°C, 9-(bromomethyl)nonadecane (4.8 g, 15 mmol) in DMF (20 mL) was added into slowly, and the mixture was stirred at 85°C for 48 h. After the mixture was cooled to room temperature, water and dichloromethane (DCM) was added to wash and extract the product for three times. The separated organic layers were collected and dried over anhydrous Na_2SO_4, and the solvent was removed under reduced pressure. The product was purified by column chromatography (silica gel; petroleum ether (PE)/DCM (v: v = 3:1) as the eluent) to give **$C_{10}C_8$DPP** as an purple solid (1.58 g, yield 37%).[1]

^{1}H NMR (400 MHz, $CDCl_3$): δ ppm 8.87 (d, 2 H), 7.52 (d, 2 H), 7.26 (d, 2 H) 4.00 (d, 4H), 1.89 (s, 2 H), 1.13-1.45 (m, 64 H), 0.87 (t, 12H). MALDI-TOF MS: Calcd. for $C_{54}H_{88}N_2O_2S_2$ [M], Exact Mass: 860.629; Found: 860.533.

2,5-Bis(2-octyldodecyl)-3,6-bis(5-(trimethylstannyl)thiophen-2-yl)-2,5-dihydropyrrolo[3,4-c]pyrrole-1,4-dione (DPP-Sn)

$C_{10}C_8$DPP (0.43 g, 0.5 mmol) was dissolved in 20 mL of the freshly distilled THF under N_2 protection. This solution was cooled down to -78°C and lithium diisopropylamine (LDA) (0.6 mL, 1.2 mmol, 2.0 M in THF) was added dropwise. After stirring at -78°C for 1 h, trimethyltin chloride solution (1.5 mL, 1.5 mmol, 1M in THF) was added rapidly into the reaction mixture. The mixture was allowed to warm to room temperature and stirred overnight. The reaction was quenched with 20 mL of cold water and extracted with Et_2O for three times. The organic extraction was washed with water twice and then dried with anhydrous Na_2SO_4. After the removal of the solvent under vacuum, the residue was purified by reverse phase column chromatography (C-18: DCM: ACN 10: 90 to 30: 70), affording of **DPP-Sn** as a purple-red solid in a yield of (0.46 g, yield 78%).[1, 2]

^{1}H NMR (400 MHz, $CDCl_3$): δ ppm 8.98 (d, J = 3.6 Hz, 2H), 7.32 (d, J = 3.6 Hz, 2H), 4.05-4.03 (d, J = 7.7 Hz, 4H), 1.91 (s, 2H), 1.38-1.11 (m, 84H), 0.88-0.83 (q, J = 6.9 Hz, 12H), 0.43 (s, 16H). ^{13}C NMR (100 MHz, $CDCl_3$) δ ppm: 161.85, 145.82, 139.86, 136.15, 135.98, 135.33, 107.23, 46.16, 37.92, 31.95, 31.91, 31.40, 30.11, 29.68, 29.66, 29.64, 29.57, 29.38, 29.33, 26.43, 22.71, 22.69, 14.15, -8.05. MALDI-TOF MS: Calcd. for $C_{60}H_{104}N_2O_2S_2Sn_2$ [M], Exact Mass: 1188.558; Found: 1188.332.

PDPP-Pyi

To a mixture of **DPP-Sn** (178 mg, 0.15 mmol), 3,6-dibromopyridazine (35.7 mg, 0.15 mmol) and $Pd(PPh_3)_4$ (6.0 mg), degassed toluene solution (5 mL) and DMF (0.5 mL) was added. The mixture was stirred at 115°C for 18 h, after which it was precipitated in methanol and filtered through a Soxhlet thimble. The polymer was extracted subsequently with acetone, hexane and chloroform. The chloroform fraction was concentrated and re-precipitated in methanol. Thus purified polymer was collected by filtering and dried in a vacuum oven to yield PDPP-Pyi (116 mg, yield 82%) as a blue-green solid.

^{1}H NMR (400 MHz, $CDCl_3$): δ ppm 9.42 (br), 8.91(br), 7.62 (br), 4.12-3.58 (m), 2.20 (br), 1.25-1.19 (m), 0.83 (br). GPC (THF): M_n = 52.9 kDa, PDI = 2.65. Elemental analysis calcd. for $C_{59}H_{90}N_4O_2S_2$: C 74.15%, H 9.66%, N 5.96%, S 6.82%; Found: C 73.91%, H 9.73%, N 5.85%, S 6.41%.

PDPP-Pya

The same synthetic and purification procedures to **PDPP-Pyi** were used for the preparation of **PDPP-Pya** by Stille coupling copolymerization of DPP-Sn (178 mg, 0.15 mmol) and 2,5-dibromopyrazine (35.7 mg, 0.15 mmol). Yield: (125 mg, yield 84%). ^{1}H NMR (400 MHz, $CDCl_3$): δ ppm 9.00 (br), 8.42(br), 7.83 (br), 4.10-3.47 (m), 2.24 (br), 1.25-1.15 (m), 0.84 (br). GPC (THF): M_n = 64.8 kDa, PDI = 1.91. Elemental analysis calcd. for $C_{59}H_{90}N_4O_2S_2$: C 74.15%, H 9.66%, N 5.96%, S 6.82%; Found: C 74.11%, H 9.64%, N 5.70%, S 6.39%.

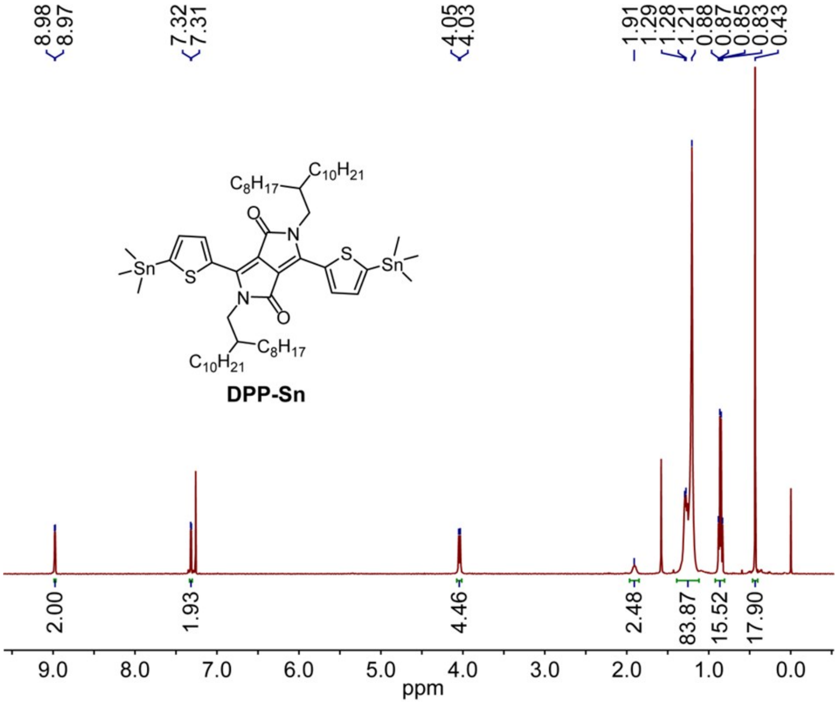

Fig. S1. ^{1}H NMR spectrum of **DPP-Sn** in $CDCl_3$.

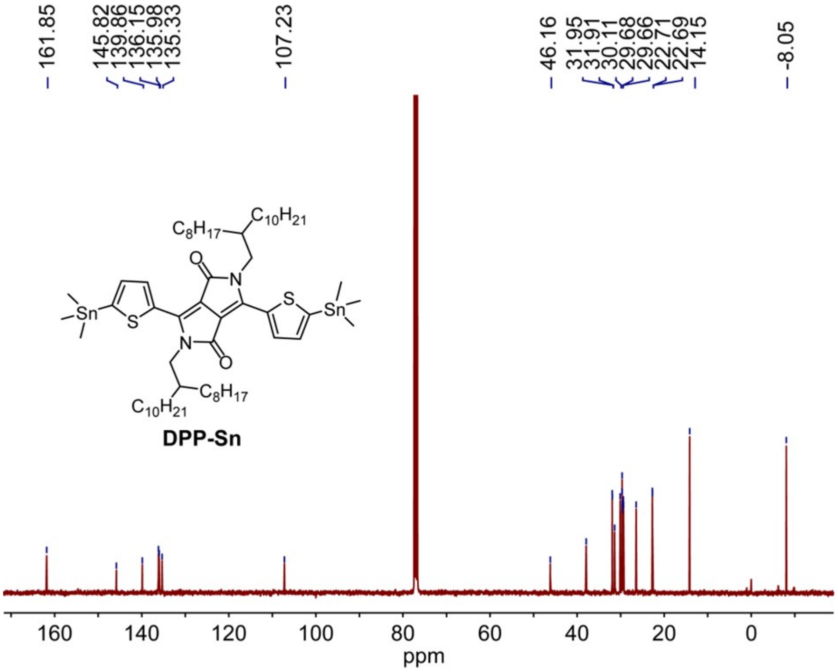

Fig. S2. ^{13}C NMR spectrum of **DPP-Sn** in $CDCl_3$.

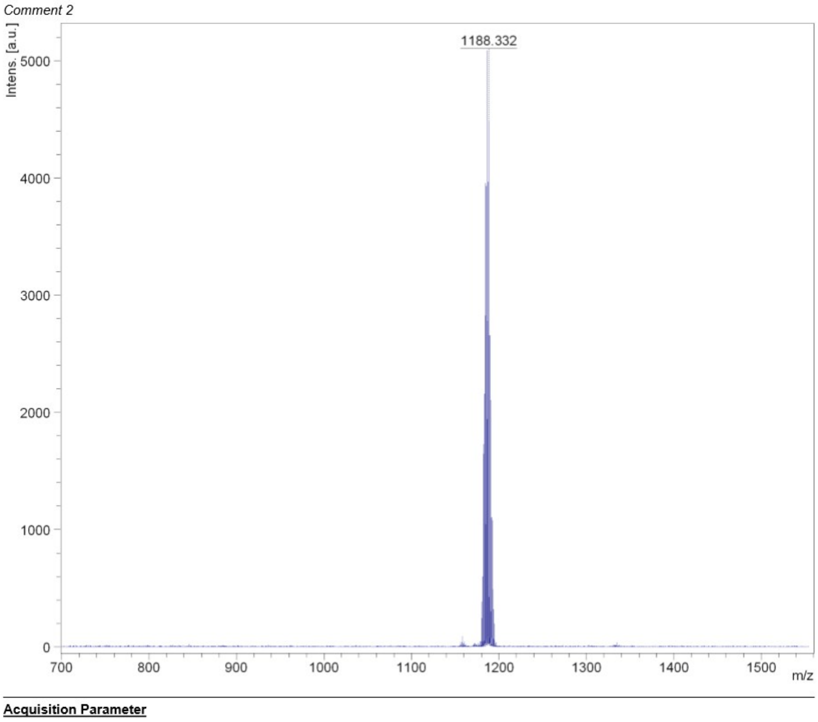

Fig. S3 MALDI-TOF MS spectrum of **DPP-Sn**.

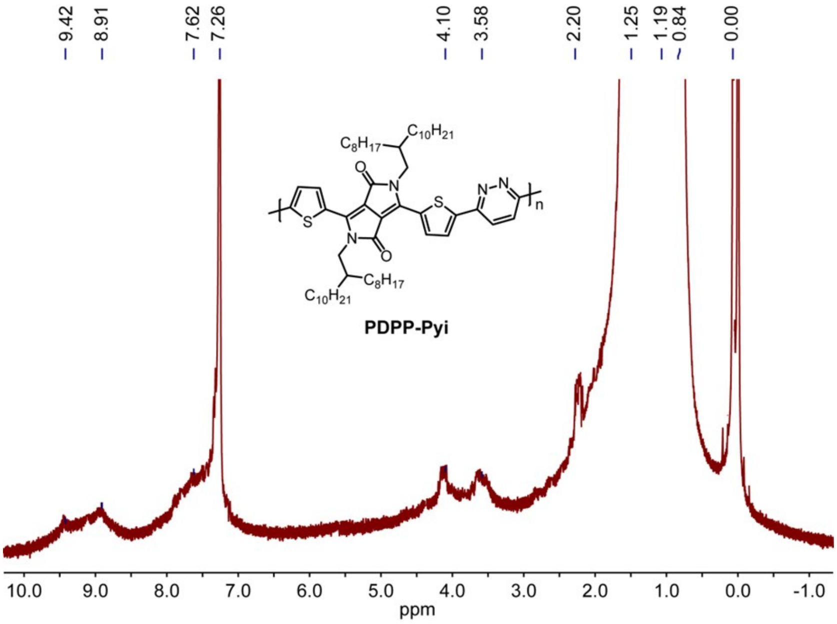

Fig. S4. ^{1}H NMR spectrum of **PDPP-Pyi** in $CDCl_3$.

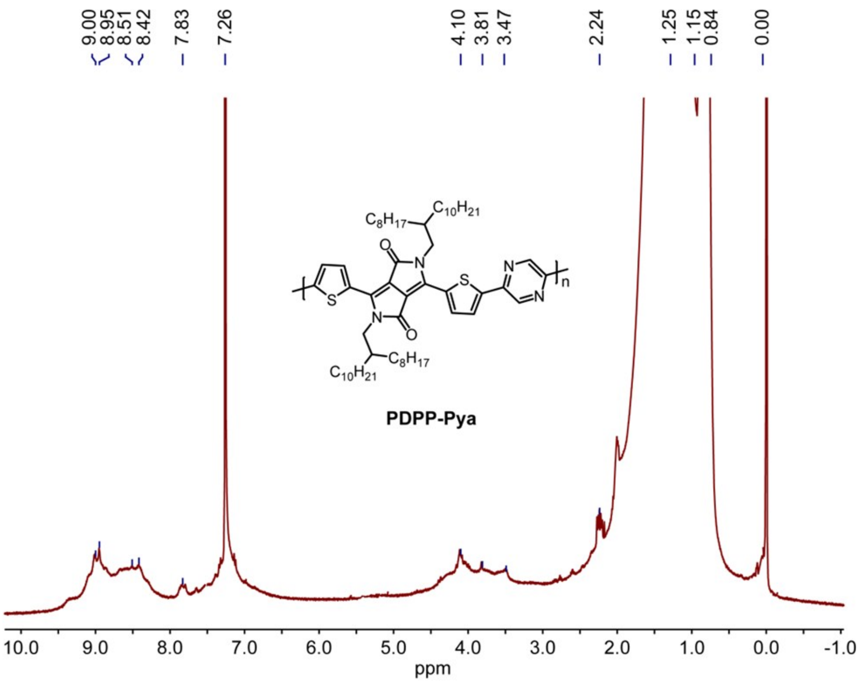

Fig. S5. ^{1}H NMR spectrum of **PDPP-Pya** in $CDCl_3$.

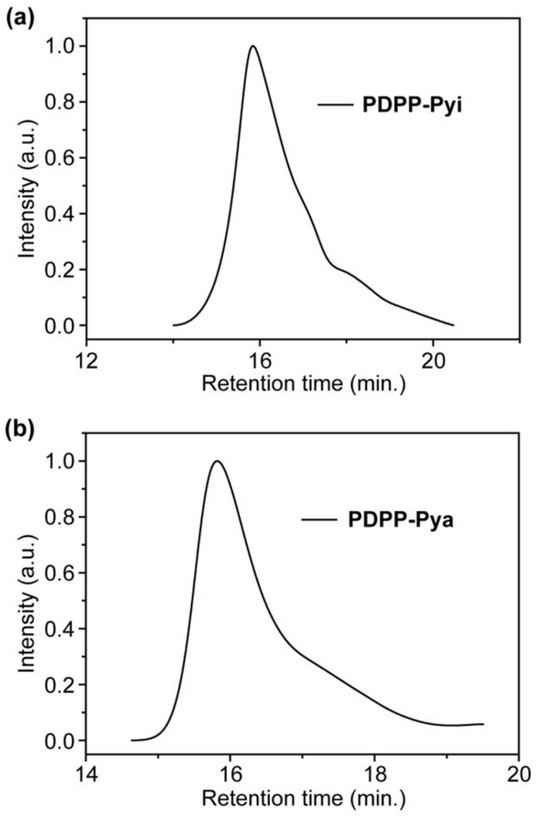

Fig. S6. GPC spectra of **PDPP-Pyi** (a) and **PDPP-Pya** (b).

4. Thermal properties

Thermogravimetric analysis (TGA) was performed to study the thermal properties of the polymers on a Shimadzu DTG-60H thermogravimetric analyses at a heating rate of 10°C/min under a nitrogen atmosphere. Differential scanning calorimetry (DSC) analyses were performed on a Shimadzu DSC-60A instrument under a heating rate of 10°C/min and a nitrogen flow rate of 20 cm^3/min. T_ds were recorded when the weight loss reaches 5%.

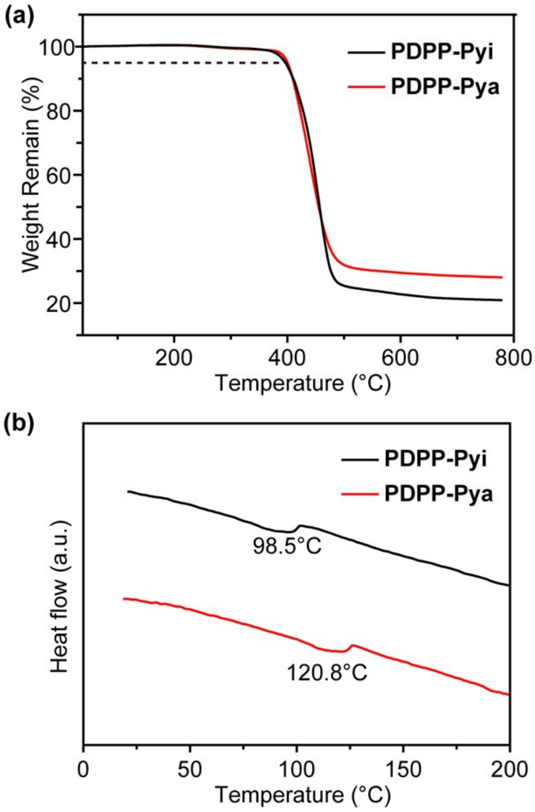

Fig. S7. TGA (a) and DSC curves (b) of **PDPP-Pyi** and **PDPP-Pya**.

5. Photophysical and Electrochemical Properties.

Photophysical properties were investigated by UV-vis absorption spectra, which were performed on a Jasco V-750 spectrophotometer. Electrochemical properties of **PDPP-Pyi** and **PDPP-Pya** were investigated by cyclic voltammetry (CV) measurements[3], which were carried out at room temperature on a CHI660E system in a typical there-electrode cell with a working electrode (glass carbon), a reference electrode (Ag/Ag$^+$), and a counter electrode (Pt wire) in an acetonitrile solution of n-$\mathrm{Bu_4NPF_6}$ (0.1 M) at a sweeping rate of 100 mV/s. The thin solid film of the compound was solution deposited on the surface of the glass carbon working electrode for the CV measurements and the CV curves were calibrated using ferrocene/ferrocenium (Fc/Fc$^+$) redox couple (4.8 eV below the vacuum level) as the internal standard. The highest occupied molecular orbital (HOMO) energy level (E_{HOMO}) was calculated according to: $E_{\mathrm{HOMO}} = \text{-e}\ (Eox\ onset + 4.80\ \mathrm{V})$, where Eox onset is the onset potential of the oxidation wave. The lowest unoccupied molecular orbital (LUMO) energy level (E_{LUMO}) was deduced by: $E_{\mathrm{LUMO}} = E_{\mathrm{HOMO}} + E_{\mathrm{g}}$, where E_{g} is the optical bandgap.

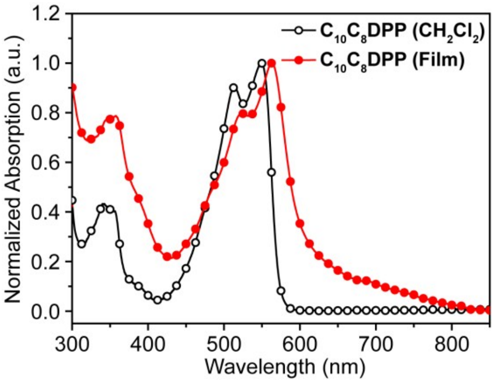

Fig. S8. Normalized absorption spectra of $\mathbf{C_{10}C_8DPP}$ in dilute $\mathrm{CH_2Cl_2}$ solution and thin film.

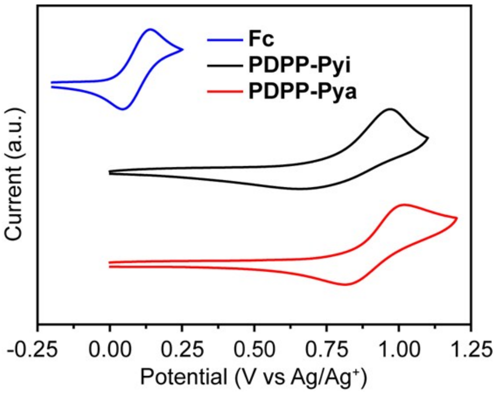

Fig. S9. Cyclic voltammograms of the polymers of **PDPP-Pya** and **PDPP-Pyi**.

6. Theoretical calculations

Density functional theory (DFT)[4] computations were carried out for structure optimizations and vibrational analyses of the monomers and oligomers on Gaussion 09 program package. The ground state (S_0) geometries of the molecules were optimized by the Becker's three-parameter exchange functional along with the Lee Yang Parr's correlation functional (B3LYP) with 6-31G (d) basis sets; the optimized stationary point was further characterized by harmonic vibrational frequency analysis to ensure that real local minima were reached. Nonbonding covalent interaction analysis (NCI)[4] was adopted to investigate the intramolecular interactions using Multiwfn version 3.3 software based on the optimized molecular structures at S_0. NCI isosurface plots were performed with color scaling that the dark blue color represents an attractive interaction, while dark red color represents repulsive interactions. Plotted isosurfaces were demonstrated with reduced density gradient (RDG) of 0.5 and $-0.5 < \mathrm{sign}(\lambda_2)\rho < 0.5$, where $\mathrm{sign}(\lambda_2)$ means the sign of the second largest eigenvalue of Hessian and ρ represents the electron density.

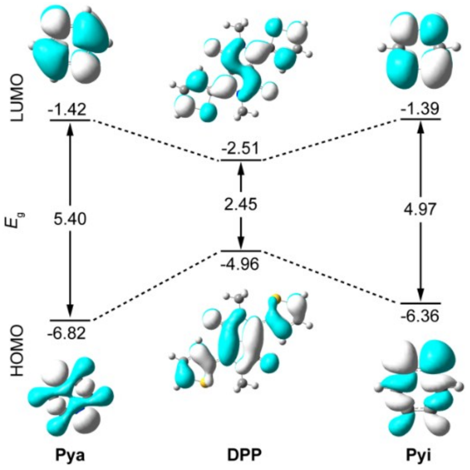

Fig. S10. DFT-calculated HOMO, LUMO, bandgap (E_g), and frontier orbital distributions of the comonomers of **Pya**, **DPP** and **Pyi** (the isosurface value is 0.02).

Table S1. Photophysical and electrochemical properties of the mA-wA polymers.

Polymer	M_n (kDa)	PDI	T_d/T_g (°C)	λ_{abs} (nm)		E_g^{opt}	CV (eV)	
				DCM	Film	(eV)	HOMO	LUMO
PDPP-Pyi	52.9	2.65	397/98.5	736	743	1.51	-5.47	-3.96
PDPP-Pya	64.8	1.91	392/120.8	790	805	1.44	-5.56	-4.12

7. Organic field effect transistor (OFET) device preparation and characterization

Glass or commercially available polyethylene terephthalate (PET) sheets with a thickness of 200 μm were used as substrates. The substrates were cleaned subsequently using deionized water, alcohol, and rinsed in acetone and dried by nitrogen before device fabrication. **PDPP-Pya** and **PDPP-Pyi** were dissolved in chlorobenzene (CB) with a concentration of 4.0 or 5.0 mg/mL, respectively. These polymer solutions were spin-coated onto the glass or PET sheets with a pre-patterned 15 nm-thick gold source and drain electrodes (channel width: channel length = 10) at 2500 rpm. Polymethyl methacrylate (PMMA) dissolved in *n*-butyl acetate (60 mg/mL) was spin-coated above the active layer as the dielectric layer and dried at 90ºC for 30 min, giving a 900 nm-thick film with a capacitance of ~3.2 nF cm^{-2}. To complete the fabrication, 80 nm thick of aluminum was thermally deposited through a shadow mask as the gate electrode. The field-effect characteristics of the top-gate/bottom-contact (TGBC) OFET devices were measured in air using a Keithley 4200 SCS semiconductor parameter analyzer.

Table S2. OFET performance of the mA-wA polymers.

Polymer	Substrate	Mobilities [cm^2 V^{-1} s^{-1}][a]		I_{on}/I_{off}		V_T [V][b]	
		μ_h	μ_e	*p*	*n*	*p*	*n*
PDPP-Pyi	PET[c]	5.20×10^{-4} (2.0×10^{-4})[e]	4.75×10^{-4} (1.8×10^{-4})[e]	10^2	10^1	-10.8,	37.5
		1.70×10^{-4} (1.6×10^{-4})[f]	5.90×10^{-5} (4.3×10^{-5})[f]	10^2	10^1	-10.8,	37.5
	Glass[d]	1.03×10^{-4} (1.0×10^{-4})[e]	1.46×10^{-4} (1.2×10^{-4})[e]	10^2	10^1-10^2	-26.2,	38.8
PDPP-Pya	PET[c]	0.16 (0.14)[e]	0.11 (0.10)[e]	10^3-10^4	10^1-10^2	-22.2,	44.7
		0.15 (0.12)[f]	0.043 (0.038)[f]	10^3-10^4	10^1-10^2	-22.2,	44.7
	PET[d]	0.26 (0.23)[e]	0.32 (0.28)[e]	10^1-10^2	10^1-10^2	-23.3,	36.5
	Glass[d]	0.39 (0.27)[e]	0.30 (0.26)[e]	10^3-10^4	10^3-10^4	-47.1,	45.4

[a] The highest mobilities and average mobilities (in parentheses) from at least five devices.

[b] The average threshold voltage (V_T) is calculated from the saturation regime.

[c] The concentration of polymer solution is 4.0 mg/mL.

[d] The concentration of polymer solution is 5.0 mg/mL.

[e] The carrier mobility (μ) was calculated from saturation region.

[f] The carrier mobility (μ) was calculated from linear region.

8. Microstructure Studies

The microstructures of the mA-wA polymers in solid film were investigated by the grazing incidence wide-angle X-ray scattering (GIWAXS). These 2D-GIWAXS measurements were performed at the 8ID-E beamline at the Advanced Photon Source (APS), Argonne National Laboratory, United States. Typical GIWAXS patterns were taken at an incidence angle of 0.13°, which was above the critical angles of neat polymers and below the critical angle of silican wafer substrate. Consequently, the entire structure of thin films can be detected. In addition, the qy linecut was obtained from a linecut across the reflection beam center, while the q_z linecut was achieved by a linecut at $q_y = 0$ Å^{-1}. Atomic force microscopy studies of thin films were performed with Cypher S microscope (Asylum Research, Oxford instruments) at tapping mode under ambient conditions using silicon cantilever (AC240TS-R3) with a resonant frequency around 70 kHz.

Table S3 Grazing incidence wide-angle X-ray scattering parameters of two polymers in film.

Polymer	Lamellar stacking		π-stacking	
	d (Å)	L_C (Å)	d (Å)	L_C (Å)
PDPP-Pyi	22.7	46.6	3.8	7.1
PDPP-Pya	19.6	77.6	3.8	10.4

Reference

1. T. J. Aldrich, A. S. Dudnik, N. D. Eastham, E. F. Manley, L. X. Chen, R. P. H. Chang, F. S. Melkonyan, A. Facchetti and T. J. Marks, Macromolecules, 2018, 51, 9140-9155.
2. T. Hasegawa, M. Ashizawa, J. Hiyoshi, S. Kawauchi, J. Mei, Z. Bao, H. Matsumoto, *Polym. Chem.* **2016**, *7*, 1181-1190.
3. Z. C. Chen, J. Li, M. G. Li, C. L. Chen, S. Xu, X. X. Tang, L. F. Chen, R. F. Chen and W. Huang, *Org. Lett.*, **2018**, 20, 6376-6379.
4. Y. F. Cheng, Y. Y. Qi, Y. T. Tang, C. Zheng, Y. F. Wan, W. Huang and R. F. Chen, *J. Phys. Chem. Lett.*, **2016**, 7, 3609-3615.